

ChIP-Seq of transcription factors predicts absolute and differential gene expression in embryonic stem cells

Zhengqing Ouyang^a, Qing Zhou^b, and Wing Hung Wong^{c,1}

^aDepartment of Biology and ^cDepartments of Statistics, Health Research and Policy, and Biology, Stanford University, Stanford, CA 94305; and ^bDepartment of Statistics, University of California, Los Angeles, CA 90095

Edited by Terry Speed, University of California, Berkeley, CA, and accepted by the Editorial Board September 25, 2009 (received for review May 5, 2009)

Next-generation sequencing has greatly increased the scope and the resolution of transcriptional regulation study. RNA sequencing (RNA-Seq) and ChIP-Seq experiments are now generating comprehensive data on transcript abundance and on regulator–DNA interactions. We propose an approach for an integrated analysis of these data based on feature extraction of ChIP-Seq signals, principal component analysis, and regression-based component selection. Compared with traditional methods, our approach not only offers higher power in predicting gene expression from ChIP-Seq data but also provides a way to capture cooperation among regulators. In mouse embryonic stem cells (ESCs), we find that a remarkably high proportion of variation in gene expression (65%) can be explained by the binding signals of 12 transcription factors (TFs). Two groups of TFs are identified. Whereas the first group (*E2f1*, *Myc*, *Mycn*, and *Zfx*) act as activators in general, the second group (*Oct4*, *Nanog*, *Sox2*, *Smad1*, *Stat3*, *Tcfcp2l1*, and *Esrrb*) may serve as either activator or repressor depending on the target. The two groups of TFs cooperate tightly to activate genes that are differentially up-regulated in ESCs. In the absence of binding by the first group, the binding of the second group is associated with genes that are repressed in ESCs and derepressed upon early differentiation.

ChIP binding | pluripotency | RNA-Seq | transcription regulation

The recent development of ultra-high-throughput RNA sequencing (RNA-Seq) technology holds the promise to provide more accurate gene expression measurements (1, 2). Compared with microarray, RNA-Seq is able to measure absolute concentration of transcripts (1). Meanwhile, chromatin immunoprecipitation (ChIP) coupled with microarray (ChIP-chip) or sequencing (ChIP-Seq) technologies have been developed to identify whole-genome localization of protein–DNA binding sites (3, 4). These data sets provide the raw materials to study the regulatory functions of transcription factors (TFs) on gene expression.

Predictive modeling (such as regression) is a statistical strategy to predict an outcome from one or more explanatory variables (predictors). In the study of transcriptional regulation, a predictive model can be constructed in which the gene expression profile under a certain condition is regarded as the response variable and various features related to TFs are taken as the predictors. Examples of such features include counts of motifs recognized by the TFs (5), sum of motif occurrences weighted by their distances from the target gene (6), motif scores based on position-specific weight matrices (7), and ChIP-chip log ratios (8). Most models are based on linear regression, but there are also extensions that include network component analysis (9), multivariate adaptive regression splines (10, 11), Bayesian error analysis model (12), boosting and Bayesian additive regression trees (13), partial least squares (14), motif expression decomposition (15), and further generalizations to pairwise interactions between TFs (6, 10, 11). Thus far, the fraction of variation in gene expression (R^2) explained by TF binding has been very

moderate, varying between 9.6% and 36.9% on various datasets from yeast to human (5, 7, 10, 11), even after considering TF–TF interaction. The low R^2 reported in these studies may be due to insufficient data or suboptimal models or both. In any case, accurate quantitative modeling of expression from binding location data has not been demonstrated.

In this paper, we show that accurate quantitative modeling of gene expression data in a mouse cell type is possible provided that TF–DNA binding locations have been measured by ChIP-Seq experiments for multiple transcriptional regulators. An important first step in this analysis is to extract suitable features from the ChIP-Seq data to serve as explanatory variables in the modeling of gene expression. From each TF, we construct a TF association strength (TFAS) for each gene by computing the weighted sum of the corresponding ChIP-Seq signal strength, where the weights reflect the proximity of the signal to the gene. The use of TFAS as a predictor variable allows us to explain a much higher proportion of gene expression variation than traditional predictors, such as the binary indicators of whether the gene is the closest gene to a ChIP-Seq peak.

Although high predictive power is a desirable property, it is important that a model has enough interpretability so that it offers insight on the regulatory roles of the TFs. One major concern is the modeling of combinatorial regulation in an efficient manner. Traditional linear prediction models are inadequate in this regard in the sense that the best linear model is represented by a single linear combination of the TF-specific predictors. If the coefficient for a TF is positive, then this model implies that the binding of this TF always results in up-regulation of the target gene; i.e., it can only serve as a positive regulator. Conversely, if the coefficient is negative, then its effect is always to repress transcription. However, it is known that a TF may contribute to the activation of some of its target genes while, at the same time, also participate in the repression of other target genes. The divergent regulatory effects of the TF may be due to differences in the binding of cofactors and/or the chromatin context. Such divergent effects are difficult to model, and current methods are limited to very low-order interactions of TFs (16). An additional difficulty of linear regression arises when the predictors are highly correlated. Since two or more TFs may cooperate to regulate many genes, we expect that the corresponding TFASs will vary in a coordinated manner across different genes; i.e., they are correlated as predictor variables. In

Author contributions: Z.O. and W.H.W. designed research; Z.O., Q.Z., and W.H.W. performed research; Z.O., Q.Z., and W.H.W. analyzed data; and Z.O. and W.H.W. wrote the paper.

The authors declare no conflict of interest.

This article is a PNAS Direct Submission. T.S. is a guest editor invited by the Editorial Board. Freely available online through the PNAS open access option.

¹To whom correspondence may be addressed at: Department of Statistics, Stanford University, 390 Serra Mall, Stanford, California 94305. E-mail: whwong@stanford.edu.

This article contains supporting information online at www.pnas.org/cgi/content/full/0904863106/DCSupplemental.

Downloaded by guest on June 1, 2021

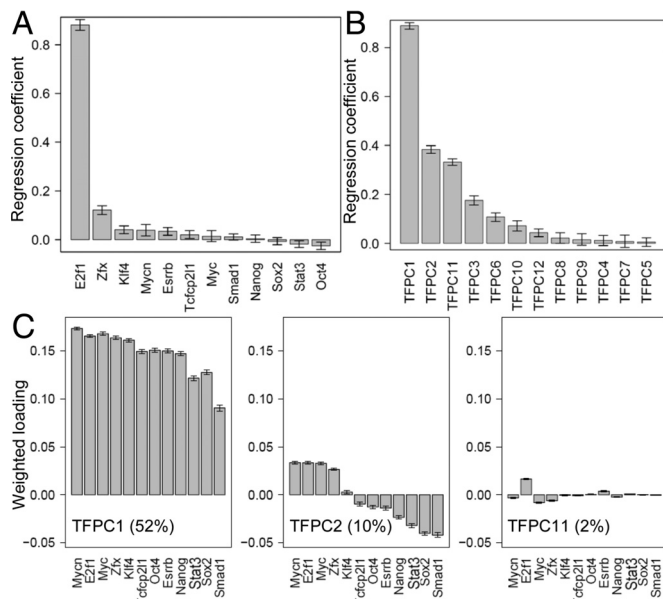


Fig. 3. TFPCs capture the roles of TFs. (A) Regression coefficients of the model using individual TFAs as predictors. (B) Regression coefficients using TFPCs as predictors. (C) Loadings of TFs in the top three selected TFPCs, weighted by the fractions of variance in TFAs explained by the TFPCs. The error bars give the 95% bootstrap confidence intervals.

the roles of individual TFs are implicated in the top TFPCs with relatively larger regression coefficients (Fig. 3B). We plotted the loadings of the individual TFs in the top TFPCs, weighted by the fractions of variance in TFAs explained by the TFPCs (Fig. 3C), which approximately reflect the relative importance of the roles of the individual TFs. Bootstrap estimation of the 95% confidence intervals indicates that the loadings are robust (SI Text). Importantly, key regulators such as *Oct4* and *Nanog* have significant loadings in the top TFPCs, and hence their importance is not masked by the effect of *E2f1*. In TFPC1 (accounting for 52% of the variance in TFAs), all of the 12 TFs have positive loadings, indicating that their primary roles are activating gene expression. In TFPC2 (accounting for 10% of the variance in TFAs), the loadings of *E2f1*, *Myc*, *Mycn*, and *Zfx* (group I TFs) are positive, while those of *Oct4*, *Nanog*, *Sox2*, *Smad1*, *Stat3*, *Tcfcp2l1*, and *Esrrb* (group II TFs) are negative, suggesting that the latter group may play a role as repressors for genes associated with high TFPC2 values. TFPC11 (accounting for 2% of the variance in TFAs) is dominated by *E2f1*, suggesting that a small percentage of genes may be activated by *E2f1* alone, or by other TFs not studied here. This analysis reveals diverse roles of the TFs. We speculate that the group I TFs activate gene expression in general, while the group II TFs may activate or repress gene expression depending on the targets. This is consistent with the reported experimental result that *E2f1* binding is proximate to the TSSs of a large number of highly expressed genes, especially those cell cycle regulated genes needed for self-renewal (27). *Myc* occupancy is close to TSSs and is associated with large scale modification of chromatin structure (28, 29). *Oct4* and *Nanog* are associated with multiple repression complexes such as the Polycomb, NuRD, Sin3A and Pml complexes (30–32), in addition to their well known activation roles in ESCs.

We next show that the regulatory rules for differential gene expression can be re-written as combinations of the group I and group II TFs. Mathematically, we transform TFPCs by: $g_1 = \frac{1}{2}(TFPC1 + TFPC2)$, $g_2 = \frac{1}{2}(TFPC1 - TFPC2)$ and $g_3 = TFPC11$. Roughly speaking, g_1 and g_2 are combinations of the group I TFs and group II TFs, respectively, and g_3 represents

Table 2. Experimental validation by the *Esrrb* RNAi knockdown data (18)

Gene symbol	FC	Gene symbol	FC
ES-Up- <i>Esrrb</i> -bound		ES-Down- <i>Esrrb</i> -bound	
<i>Ndg2</i>	0.62	<i>Trpc3</i>	2.12
<i>Icam1</i>	0.34	<i>Zfp1</i>	2.63
<i>Klk1</i>	0.93	<i>Sema3f</i>	4.29
<i>Mreg</i>	0.62	<i>Gpr124</i>	3.54
<i>Ldhh</i>	0.50	<i>St6galnac4</i>	1.14
<i>Mybl2</i>	0.79	<i>Ryr2</i>	0.98
<i>6430514L14Rik</i>	1.16	<i>G0s2</i>	2.09
<i>Lrrc2</i>	0.22	<i>Apobec2</i>	0.80
<i>Myplf</i>	0.71	<i>Pxmp3</i>	1.08
<i>Sept1</i>	0.73	<i>Evx1</i>	1.16

FC, fold change of gene expression between the mean level of the day 6 and day 7 samples and the level of the day 0 sample, after RNAi knockdown of *Esrrb*.

E2f1. Then the regulatory rules can be reexpressed as follows. Uniform Low: $g_1 + g_2 < -0.77$ AND $g_3 < 0.25$; ES Down: $-0.77 \leq g_1 + g_2 < 0.06$ AND $g_2 - g_1 > -1.47$; Uniform High: $g_1 + g_2 \geq 0.06$ AND $g_1 - g_2 \geq 0.45$; and ES Up: $g_1 + g_2 \geq 0.75$ AND $g_2 - g_1 > 0.64$. It can be seen that $(g_1 + g_2)$ increases in the order of Uniform Low, ES Down, Uniform High, and ES Up, which means the cooperation between the group I and II TFs becomes more and more extensive. Notably, although both the Uniform High and ES Up gene sets are highly expressed in ESCs, we found that the former favors the group I TFs while the latter favors the group II TFs as reflected by the signs of $(g_1 - g_2)$. And although both the Uniform Low and ES Down gene sets are lowly expressed in ESCs, genes in the former may simply not be bound by any of the TFs, while genes in the latter show detectable TF binding events and the group II TF binding is preferred. Recall that the group II TFs include typical ESC-specific regulators such as *Oct4*, *Sox2*, *Nanog*, *Stat3*, and *Esrrb*. This is consistent with the hypothesis that the group II TFs are important for the control of differential gene expression in ESCs.

As discussed in the above, group II TFs such as *Esrrb* can be either an activator (e.g., on ES Up genes) or a repressor (e.g., on ES Down genes). To test this hypothesis, we took the top 10 genes with the strongest *Esrrb* TFAS values from the correctly predicted ES Up genes, and also the same from the ES Down genes. We asked whether the knockdown of *Esrrb* expression will down-regulate the expression levels of the first group and up-regulate the expression levels of the second group, as predicted by our model. We obtained the relevant expression data after *Esrrb* knockdown from ref. 18, which is an independent data set not used in the construction of our model. As shown in Table 2, the expression levels of 9 of the 10 ES-Up-*Esrrb*-bound genes decreased with the knockdown of *Esrrb*, and 8 of the 10 ES-Down-*Esrrb*-bound genes increased. This provides an independent, experimental validation of the model.

Combinatorial Gene Regulation of ESC Pluripotency. The Polycomb Repressive Complex 2 (PRC2) plays an important role in maintaining ESC pluripotency by gene repression (30, 31). The ChIP-Seq data of *Suz12*, a key subunit of PRC2, is available along with the 12 sequence-specific TFs (20). But because it does not bind DNA sequences directly, we did not include it in the above analysis. Instead, we studied the overlaps between its binding targets and the four gene sets, as well as the predicted gene sets based on the inferred regulatory rules. We identified 1938 *Suz12* bound genes with $TFAS \geq 2$. *Suz12* bound genes are strongly enriched in the ES Down gene sets (Enrichment level

$R = 3.9$, P value $= 6 \times 10^{-119}$), while not enriched in any of the other three sets (Fig. S4 A–D), confirming its association with ESC-repressed genes. They are also enriched in the predicted set of ES Down genes ($R = 3.2$, P value $= 7 \times 10^{-86}$), suggesting potential interaction between *Suz12* and the sequence-specific TFs. This is consistent with the observation that a significant subset of PRC2 target genes are co-occupied by the ESC regulators *Oct4*, *Sox2* and *Nanog* (31). It is interesting to note that there are 71 predicted ES Down genes which are not in the observed ES Down gene set but are actually bound by *Suz12* (Table S3). Some of them may be up-regulated in certain cell differentiation lineages (and thus become ES Down) not covered in this analysis. For example, the *Olig1* and *Olig2* genes are important for neural progenitor cells to develop into mature neurons, and are up-regulated in neural progenitor cells versus ESCs (30).

The above analyses suggest combinatorial roles of the TFs on regulating ESC pluripotency. *E2f1*, *Myc*, *Mycn*, and *Zfx* may contribute to rapid proliferation of ESCs. Since they maintain their expression when ESCs differentiate to early differentiation stages (data from the RNA-Seq and the array profiles), they may continue to activate the expression of genes that are essential for proliferation. The group II TFs, on the other hand, maintain ESC pluripotency through activating genes that are otherwise silent in differentiated cells. The maintenance of ESC pluripotency also involves inhibition of genes expressed in differentiated cells. The regulatory rules we found above suggest that the 12 TFs may interact with PRC2 to repress differentiation related genes in the absence of the group I TFs. For example, the ESC up-regulated gene *Gdf3* is bound by both the group I and II TFs (Fig. S5A), while the ESC down-regulated gene *Foxa2* is only bound by the group II TFs plus *Suz12* (Fig. S5B).

Discussion

By joint modeling of ChIP-Seq and gene expression data (RNA-Seq and microarray) we quantified the contribution of TF binding on gene expression regulation. We demonstrated that binding signals of sequence-specific TFs have remarkably high predictive power on absolute mRNA abundance. We found that gene expression indices measured by RNA-Seq have a noticeable higher correlation with TF binding than those measured by microarray.

We have studied the roles of TF binding on regulating differential gene expression in ESCs. We found that a few simple rules defined by the combinations of TFs are able to summarize the major modes of cooperation among these TFs. The first principal component of the ChIP-Seq signal is essentially uniform across all 12 TFs studied here. This is consistent with the finding that many genomic loci are bound by a large number of different TFs (33, 34). We found that some TFs (group II TFs) have divergent roles in regulating gene expression, i.e., they contribute to activation on some genes but repression on other genes. Understanding why they act as both activators and repressors will help to illustrate the mechanism of pluripotency. Also, the interaction between sequence-specific TFs and PRC2 should be further investigated to clarify how PRC2 recognizes and silences its target genes.

The approach of first extracting characteristic TFAS patterns and then select among them the ones with good predictive power can be generalized. Here we have used principal component analysis for simplicity, but other methods such as k -means clustering can also be considered. The basic feature space can be expanded, so that instead of defining one TFAS variable for each TF, one may construct predictor variables designed to capture more fine-scaled co-localization among different TFs. While the simple approach offered here seems already effective in quantitative modeling of gene expression in ESCs based on ChIP-Seq data, further refinement and extension of the basic approach

may be needed to fully extract the rich information in these massive data sets.

Materials and Methods

ChIP-Seq and Gene Expression Data. The ChIP-Seq binding peak data of the 12 TFs in mouse ESCs were obtained from Chen et al. (20). The peaks in the neighborhood of peaks of a control GFP (20) were filtered out to eliminate false positives due to nonspecific binding. We obtained mapped mRNA sequencing data for mouse ESCs and EBs (2). The gene expression values of the sequencing data were calculated by modifying the code of the ERANGE program, based on the RPKM definition (1). The RNA-Seq expression profiles of mouse brain, liver and muscle were used for comparison (1). The Affymetrix MOE430 V2 array profiles of the *Oct4* sorted series were obtained from Zhou et al. (21), in which 8 are *Oct4*-high samples (three ESC profiles and five EB profiles with cells selected by high *Oct4* expression) and the rest are *Oct4*-low samples (eight EB profiles with cells selected by low *Oct4* expression). The Affymetrix MOE430 AB array profiles of the RA induction and *Esrrb* RNAi knockdown series are from Ivanova et al. (18). Our analysis focused on the well annotated mouse Refseq genes ($N \approx 19,000$). The genomic coordinates of the mm8 mouse Refseq genes were obtained from the UCSC GoldenPath database.

TF Association Strength. Binary. Traditionally, a TF binding peak is usually associated with a gene so that the distance between the peak and the gene (usually the TSS) is the nearest out of all Refseq genes (35). Denoting the binary TFAS as a_{ij} , a_{ij} is equal to 1 if gene i is associated with a peak of TF j ; otherwise a_{ij} is equal to 0. This approach does not take into account the intensity of the peaks and the relative distance between peaks and genes.

Continuous. We integrate the peak intensity and the proximity to genes to define the association strength between a TF and a gene. We assume that the association strength of TF j on gene i is a weighted sum of intensities of all of the peaks of TF j :

$$a_{ij} = \sum_k g_k e^{-d_k/d_0},$$

where g_k is the intensity (number of reads aligned to the coordinate) of the k th binding peak of the TF j , d_k is the distance (number of nucleotides) between the TSS of gene i and the k th binding peak in the reference genome, and d_0 is a constant. In theory, the summation is over all binding peaks of a given TF. But the effect of a peak decays exponentially when d_k increases where the speed depends on d_0 . When d_k/d_0 is very large the contribution of the peak will be effectively zero. We set $d_0 = 500$ bps for *E2f1* and 5,000 bps for other TFs because *E2f1* tends to be closer to TSSs. To save computation time, we only consider peaks within a sufficiently large distance (say, 1 Mbps) of a gene. The TFAS values are then log-transformed and quantile-normalized. For N genes and M TFs the TFAS profiles are denoted by an $N \times M$ matrix A .

PC Regression. We use PCA to extract characteristic patterns (TFPCs) from the TFAS profiles of multiple TFs. After having been centered and standardized, the TFAS matrix A is decomposed by the singular value decomposition (SVD) $A = U\Sigma V^T$, where both U (an $N \times M$ matrix) and V (an $M \times M$ matrix) are orthogonal matrices, and Σ (an $M \times M$ matrix) is diagonal. The loading matrix V consists of the weights of individual TFs in the TFPCs. We denote $X = U\Sigma$, where the TFPC scores are specified. PCA has been used to capture characteristic modes of gene expression profiles, where the principal components are called eigengenes (36, 37), and to study the clustering property of TFs based on their genomic distributions (38). Here we aim to use TFPCs to predict gene expression.

Given a single condition, the gene expression is expressed by the log-linear regression model

$$\log Y_i = \mu + \sum_{j=1}^M \beta_j X_{ij} + \varepsilon_i,$$

where Y_i is the absolute expression of gene i , μ is the basal expression, X_{ij} is the score of the j th TFPC on gene i , β_j is the regression coefficient of the j th TFPC, and ε_i is a gene-specific error term. To avoid taking the logarithm of zero, a small positive constant is added to Y_i . In this model, each TF contributes to the prediction through the TFPCs. Thus the same TF can have positive effect on gene expression through one TFPC and negative effect through a different TFPC. This allows interpreting a TF as both activator and repressor, depending on the TF combinations. Another advantage of using TFPCs as the predictors

is that the regression coefficients do not affect each other and each TFPC can explain a unique fraction of the variance of gene expression since the TFPCs are uncorrelated. Thus these TFPCs can be ordered in a decreasing manner by their importance for gene expression. We use the R^2 to measure how much variation in gene expression can be explained by the TF binding data. To evaluate the predictive power of the model on new datasets, we employ ten-fold cross-validation to calculate the average R^2 in the ten independent test sets which is denoted by $CV\text{-}R^2$.

Gene Selection Criteria. We apply the SVD to analyze gene expression patterns upon ESC differentiation. The top two gene expression principal components are denoted by GPC1 and GPC2. The Uniform High or Uniform Low genes are those with higher or lower 2.5% values in GPC1. The ES Up or ES Down genes are those with higher or lower 2.5% values in GPC2. The respective unions of

the four sets of genes from the RNA-Seq dataset and those from the array dataset are taken as the final gene sets (*SI Text*).

Classification Tree. We applied the CART algorithm (26) to learn a classification tree to distinguish the four gene sets using the TFPCs as predictors. We use 10-fold cross-validation to choose the most parsimonious tree with a CV error within one standard error of the minimum (26). For detailed description of the CART algorithm, see *SI Text*.

ACKNOWLEDGMENTS. We thank Michael Zhang for a careful reading of the manuscript and Zhen-Su She for comments. This work was supported by National Institutes of Health Grants R01HG004634 and R01HG003903, National Science Foundation Grant DMS-0805491, and California Institute for Regenerative Medicine (CIRM) Grant RC1-00133. Z.O. thanks the CIRM for a predoctoral fellowship.

1. Mortazavi A, et al. (2008) Mapping and quantifying mammalian transcriptomes by RNA-Seq. *Nat Methods* 5:621–628.
2. Cloonan N, et al. (2008) Stem cell transcriptome profiling via massive-scale mRNA sequencing. *Nat Methods* 5:613–619.
3. Boyer LA, et al. (2005) Core transcriptional regulatory circuitry in human embryonic stem cells. *Cell* 122:947–956.
4. Johnson DS, Mortazavi A, Myers RM, Wold B (2007) Genome-wide mapping of in vivo protein-DNA interactions. *Science* 316:1497–1502.
5. Bussemaker HJ, Li H, Siggia ED (2001) Regulatory element detection using correlation with expression. *Nat Genet* 27:167–171.
6. Keles S, van der Laan M, Eisen MB (2002) Identification of regulatory elements using a feature selection method. *Bioinformatics* 18:1167–1175.
7. Conlon EM, Liu XS, Lieb JD, Liu JS (2003) Integrating regulatory motif discovery and genome-wide expression analysis. *Proc Natl Acad Sci USA* 100:3339–3344.
8. Gao F, Foat BC, Bussemaker HJ (2004) Defining transcriptional networks through integrative modeling of mRNA expression and transcription factor binding data. *BMC Bioinformatics* 5:31.
9. Liao JC, et al. (2003) Network component analysis: Reconstruction of regulatory signals in biological systems. *Proc Natl Acad Sci USA* 100:15522–15527.
10. Das D, Banerjee N, Zhang MQ (2004) Interacting models of cooperative gene regulation. *Proc Natl Acad Sci USA* 101:16234–16239.
11. Das D, Nahl Z, Zhang MQ (2006) Adaptively inferring human transcriptional subnetworks. *Mol Syst Biol* 2:msb4100067.
12. Sun N, Carroll RJ, Zhao H (2006) Bayesian error analysis model for reconstructing transcriptional regulatory networks. *Proc Natl Acad Sci USA* 103:7988–7993.
13. Zhou Q, Liu JS (2008) Extracting sequence features to predict protein-DNA interactions: a comparative study. *Nucleic Acids Res* 36:4137–4148.
14. Boulesteix AL, Strimmer K (2005) Predicting transcription factor activities from combined analysis of microarray and ChIP data: A partial least squares approach. *Theor Biol Med Model* 2:23.
15. Nguyen DH, D'Haeseleer P (2006) Deciphering principles of transcription regulation in eukaryotic genomes. *Mol Syst Biol* 2:msb4100054.
16. Madar A, Bonneau R (2009) Learning global models of transcriptional regulatory networks from data. *Methods Mol Biol* 541:1–30.
17. Chambers I, Smith A (2004) Self-renewal of teratocarcinoma and embryonic stem cells. *Oncogene* 23:7150–7160.
18. Ivanova N, et al. (2006) Dissecting self-renewal in stem cells with RNA interference. *Nature* 442:533–538.
19. Wang J, et al. (2006) A protein interaction network for pluripotency of embryonic stem cells. *Nature* 444:364–368.
20. Chen X, et al. (2008) Integration of external signaling pathways with the core transcriptional network in embryonic stem cells. *Cell* 133:1106–1117.
21. Zhou Q, Chipperfield H, Melton D, Wong WH (2007) A gene regulatory network in mouse embryonic stem cells. *Proc Natl Acad Sci USA* 104:16438–16443.
22. Irizarry RA, et al. (2005) Multiple-laboratory comparison of microarray platforms. *Nat Methods* 2:345–350.
23. Shi L, et al. (2006) The MicroArray Quality Control (MAQC) project shows inter- and intraplatform reproducibility of gene expression measurements. *Nat Biotechnol* 24:1151–1161.
24. Kuo WP, et al. (2006) A sequence-oriented comparison of gene expression measurements across different hybridization-based technologies. *Nat Biotechnol* 24:832–840.
25. Dennis G, Jr, et al. (2003) DAVID: Database for Annotation, Visualization, and Integrated Discovery. *Genome Biol* 4:P3.
26. Hastie T, Tibshirani R, Friedman JH (2001) *The Elements of Statistical Learning* (Springer, New York).
27. Bieda M, Xu X, Singer MA, Green R, Farnham PJ (2006) Unbiased location analysis of E2F1-binding sites suggests a widespread role for E2F1 in the human genome. *Genome Res* 16:595–605.
28. Guccione E, et al. (2006) Myc-binding-site recognition in the human genome is determined by chromatin context. *Nat Cell Biol* 8:764–770.
29. Kim J, Chu J, Shen X, Wang J, Orkin SH (2008) An extended transcriptional network for pluripotency of embryonic stem cells. *Cell* 132:1049–1061.
30. Boyer LA, et al. (2006) Polycomb complexes repress developmental regulators in murine embryonic stem cells. *Nature* 441:349–353.
31. Lee TI, et al. (2006) Control of developmental regulators by Polycomb in human embryonic stem cells. *Cell* 125:301–313.
32. Liang J, et al. (2008) Nanog and Oct4 associate with unique transcriptional repression complexes in embryonic stem cells. *Nat Cell Biol* 10:731–739.
33. Moorman C, et al. (2006) Hotspots of transcription factor colocalization in the genome of *Drosophila melanogaster*. *Proc Natl Acad Sci USA* 103:12027–12032.
34. Li XY, et al. (2008) Transcription factors bind thousands of active and inactive regions in the *Drosophila* blastoderm. *PLoS Biol* 6:e27.
35. Ji H, et al. (2008) An integrated software system for analyzing ChIP-chip and ChIP-seq data. *Nat Biotechnol* 26:1293–1300.
36. Holter NS, et al. (2000) Fundamental patterns underlying gene expression profiles: simplicity from complexity. *Proc Natl Acad Sci USA* 97:8409–8414.
37. Alter O, Brown PO, Botstein D (2000) Singular value decomposition for genome-wide expression data processing and modeling. *Proc Natl Acad Sci USA* 97:10101–10106.
38. Zhang ZD, et al. (2007) Statistical analysis of the genomic distribution and correlation of regulatory elements in the ENCODE regions. *Genome Res* 17:787–797.